

First lidar observations of polar mesospheric clouds and Fe temperatures at McMurdo (77.8°S, 166.7°E), Antarctica

Xinzhao Chu,¹ Wentao Huang,¹ Weichun Fong,¹ Zhibin Yu,¹ Zhangjun Wang,¹ John A. Smith,¹ and Chester S. Gardner²

Received 2 June 2011; revised 15 July 2011; accepted 23 July 2011; published 27 August 2011.

[1] We report the first lidar observations of polar mesospheric clouds (PMCs) and temperatures made with an Fe Boltzmann lidar at McMurdo, Antarctica in summer 2010–2011. Eighty-five hours of PMCs were observed between 21 Dec 2010 and 15 Feb 2011, giving an overall occurrence frequency of 29.9%. The mean PMC centroid altitude is 84.59 ± 0.17 km, confirming previous reports that clouds in the Southern Hemisphere are ~ 1 km higher than in the North. By combining the McMurdo (77.8°S) observations with those obtained at the South Pole (90°S) and Rothera (67.5°S), we find that the mean PMC altitude increases with increasing latitude with a statistically significant ascending rate of 40 ± 3 m/deg. A negative correlation is found between the daily-mean temperatures at 90 km and PMC brightness. The observations provide direct evidence that the cold phase of wave-induced temperature oscillations facilitates PMC formation and Fe depletion, supporting previous modeling results. **Citation:** Chu, X., W. Huang, W. Fong, Z. Yu, Z. Wang, J. A. Smith, and C. S. Gardner (2011), First lidar observations of polar mesospheric clouds and Fe temperatures at McMurdo (77.8°S, 166.7°E), Antarctica, *Geophys. Res. Lett.*, 38, L16810, doi:10.1029/2011GL048373.

1. Introduction

[2] Layered phenomena in the mesosphere and lower thermosphere (MLT), such as polar mesospheric clouds (PMCs) and the meteoric metal layers, not only pose interesting scientific curiosities of where they come from, how they form and why they vary, but they also serve as excellent tracers for studying the composition, thermal structure, chemistry and dynamics in the upper atmosphere. Lidar observations of PMC and Fe layers at the South Pole (90°S) and Rothera (67.5°S) have characterized these layers at two representative sites in the Southern Hemisphere [Chu *et al.*, 2003, 2006; Gardner *et al.*, 2005, 2011]. The hemispheric difference and latitudinal dependence of the mean PMC altitudes [Chu *et al.*, 2003, 2006], the depletion of Fe and Na by PMCs [Plane *et al.*, 2004; Gardner *et al.*, 2005] and the significant differences found in the Fe seasonal behavior between the South Pole and Rothera [Gardner *et al.*, 2011] are among several science discoveries that have emerged from these studies. They illustrate how observations of the PMC and metal layers

at high latitudes provide a sensitive test of the large-scale dynamics and chemistry of the upper atmosphere.

[3] Despite the success of lidar observations at the South Pole and near the Antarctic Circle at Rothera, Davis and Syowa stations [Klekociuk *et al.*, 2008; Kawahara *et al.*, 2004], a critical data gap existed in latitude between 90°S and 69°S. To help fill this gap, during the austral summer of 2010–2011, we deployed an Fe Boltzmann temperature lidar to McMurdo Station (77.83°S, 166.66°E), half way between the South Pole and the Antarctic Circle. McMurdo is located on the Ross Island at a higher magnetic latitude than either the South Pole or Rothera. This lidar was originally developed at the University of Illinois [e.g., Chu *et al.*, 2002] and deployed on several airborne campaigns in the Northern Hemisphere (1998–1999) and then to the South Pole (1999–2001) and Rothera (2002–2005). Recently the instrument was refurbished at the University of Colorado and upgraded by incorporating newly available seed-laser technologies, which improved the measurement accuracy of Fe temperatures at high temporal resolution. With the support and collaboration of the United States Antarctic Program and Antarctic New Zealand (AntNZ), the University of Colorado lidar group installed the Fe lidar into the AntNZ facility at Arrival Heights, McMurdo in Nov and Dec 2010. The lidar has full diurnal coverage and is capable of detecting PMCs and Fe layers under full sunlight. Following installation, it was operated around the clock, weather permitting, in order to acquire as many PMC observations as possible.

[4] In this paper we present the observations of PMC and Fe temperatures taken in the first summer season from Dec 2010 to Feb 2011. These data provide a good test of previous findings concerning PMC altitudes and strengthen their statistical significance in the Southern Hemisphere. By analyzing simultaneous measurements of PMC and the Fe temperatures above the clouds, we present direct evidence that cloud formation is facilitated during the cold-phase of wave-induced temperature oscillations, especially when the daily-mean temperature is relatively warm.

2. Observations

[5] PMC and Fe data were collected with resolutions of 48 m and 1 min. To be consistent with the South Pole and Rothera PMC analysis, the photon count profiles were integrated for one hour and then vertically smoothed by a Hamming window with full-width-at-half-maximum of 960 m. The criteria and procedures used to identify PMC peaks were the same as described by Chu *et al.* [2006]. Temperature derivation and error analysis are given by Chu *et al.* [2002].

[6] The first positive detection of PMC was achieved on 21 Dec 2010, and the last PMC was detected on 15 Feb

¹Cooperative Institute for Research in Environmental Sciences and Department of Aerospace Engineering Sciences, University of Colorado at Boulder, Boulder, Colorado, USA.

²Department of Electrical and Computer Engineering, University of Illinois at Urbana-Champaign, Urbana, Illinois, USA.

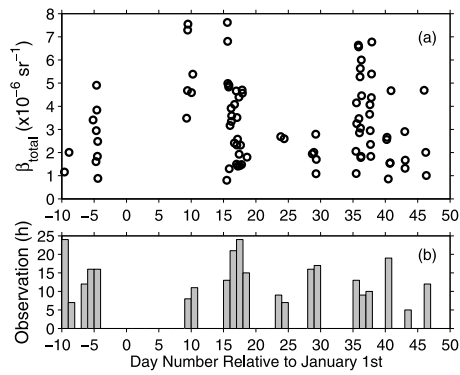


Figure 1. Seasonal variations of (a) hourly-mean PMC total backscatter coefficient and (b) lidar observational hours plotted versus day number relative to January 1st.

2011. During this 57-day period, 284 hours of lidar data were collected on 21 different days. PMCs were observed during 85 hours, giving an overall PMC occurrence frequency of 29.9%. Hourly PMC total backscatter coefficient β_{total} (see *Chu et al.* [2003] for definition) and daily observational hours are plotted against day number in Figure 1. PMC detection commenced on the summer solstice, with a single low-brightness cloud. A data gap occurred between 27 Dec 2010 and 8 Jan 2011 due to nearly two weeks of overcast skies at McMurdo. The brightest PMCs were detected on 9–10 Jan 2011 and 15 Jan 2011. Bright PMCs were also observed from 4–6 Feb 2011.

2.1. Mean Characteristics of PMC

[7] PMC mean characteristics for the 2010–2011 summer season are summarized in Table 1, along with the corresponding South Pole and Rothera data. The 85 hours of PMC observations are distributed quite evenly covering all 24 hours, so the diurnal bias in the mean characteristics is minimal. The PMC brightness at McMurdo, characterized by the total backscatter coefficient β_{total} at the wavelength of 374 nm, falls between the South Pole and Rothera values. The McMurdo β_{total} varies from 0.80×10^{-6} to $7.62 \times 10^{-6} \text{ sr}^{-1}$ with a mean of $3.30 \pm 0.19 \times 10^{-6} \text{ sr}^{-1}$. The mean width of the PMC layers at McMurdo is larger than at the South Pole, but comparable to the mean width at Rothera.

[8] The mean centroid altitude of the McMurdo PMCs is $84.59 \pm 0.17 \text{ km}$, which is mid-way between the mean altitudes of the South Pole and Rothera PMCs as illustrated in Figure 2. Also plotted are the mean altitudes of PMCs in the Northern Hemisphere (NH) obtained by various lidar observations and ground-based triangulation measurements

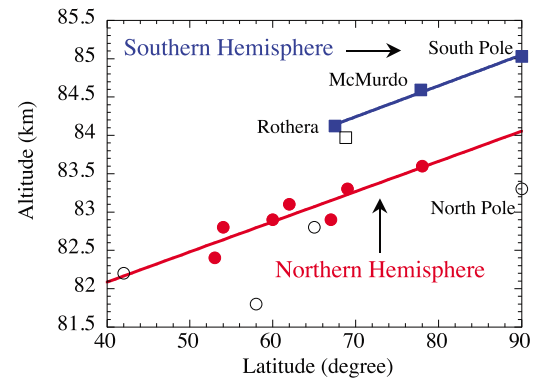


Figure 2. Comparison of the mean altitudes of PMCs versus latitude in both hemispheres. Squares are for the Southern Hemisphere and circles are for the Northern Hemisphere. Filled squares and circles indicate large data sets and are used to obtain the linear fits (solid lines) in both hemispheres. The SH fit has a slope of $40 \pm 3 \text{ m/deg}$ with a correlation coefficient of 99.76%. Open circles indicate limited data sets and are excluded from the NH fit. The Davis data point (open square, $83.97 \pm 0.10 \text{ km}$) reported by *Klekociuk et al.* [2008] is excluded from the SH fit. See *Chu et al.* [2006] and text for references.

(taken from *Chu et al.* [2006] and references therein). The McMurdo result confirms the discovery of hemispheric difference that PMCs in the Southern Hemisphere (SH) are $\sim 1 \text{ km}$ higher than their northern counterparts [*Chu et al.*, 2003, 2006]. A latitudinal dependence of PMC altitude is clearly shown in Figure 2, confirming another discovery that higher latitudes host PMCs at higher altitudes [*Chu et al.*, 2006]. If no assumption is made regarding the uncertainties of the Rothera, McMurdo and South Pole data points, a simple linear fit to the mean altitudes gives a slope of $40 \pm 3 \text{ m/deg}$, which is the ascending rate of PMC altitude with latitude in the South. The mean PMC altitudes measured by lidars at all four SH sites including Davis are consistent with this linear trend.

[9] *Chu et al.* [2006] derived a slope of $39 \pm 8 \text{ m/deg}$ for the ascending rate of PMC altitude in the North. *Lübken et al.* [2008] gave a similar slope of $43 \pm 65 \text{ m/deg}$ for the NH. *Lübken et al.* [2008] assumed that the errors of the mean PMC altitudes for the sites they analyzed were equal to the rms geophysical variabilities of the measured PMC altitudes at each site, hence the large uncertainty in the slope that they reported. We have used the standard statistical approach for calculating the error of the mean as the rms variability divided by the square root of the number of independent samples. To be conservative we assume a correlation

Table 1. Comparison of Mean PMC Characteristics at the South Pole, McMurdo and Rothera^a

Mean Characteristics	South Pole (90°S) (1999–2001)	McMurdo (78°S) (2010–2011)	Rothera (67.5°S) (2002–2005)
Total backscatter coefficient, $\beta_{\text{total}} (\times 10^{-6} \text{ sr}^{-1})$	5.45 ± 0.19 (3.73)	3.30 ± 0.19 (1.75)	2.34 ± 0.11 (1.28)
Centroid altitude, Z_C (km)	85.03 ± 0.05 (1.02)	84.59 ± 0.17 (1.59)	84.12 ± 0.12 (1.35)
Layer RMS width, σ_{rms} (km)	0.75 ± 0.02 (0.30)	0.87 ± 0.04 (0.35)	0.93 ± 0.03 (0.32)
PMC occurrence	437 h	85 h	128 h
PMC occurrence frequency	67.4%	29.9%	27.9%
PMC occurrence period	24 Nov to 24 Feb	21 Dec 2010 to 15 Feb 2011	19 Nov to 2 Feb

^aFor each parameter of β_{total} , Z_C and σ_{rms} , the first number is the mean value, the second number is the standard error of the mean, and the number in parentheses is the standard deviation of the distribution, i.e., the geophysical variability.

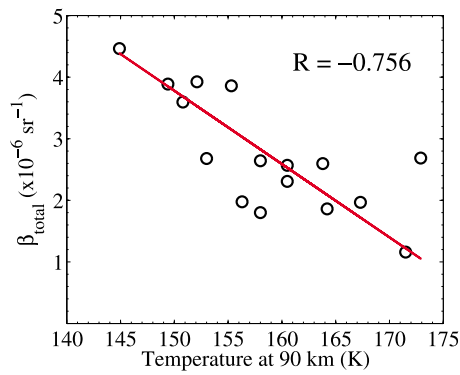


Figure 3. Correlation between daily-mean PMC total backscatter coefficient and daily-mean temperature at 90 km. The straight line is a linear regression of the form $\beta_{\text{total}}(10^{-6} \text{ sr}^{-1}) = 21.65 - 0.119T(K)$. The typical uncertainty of the daily-mean β_{total} is $\sim 0.6 \times 10^{-6} \text{ sr}^{-1}$ or less, and the typical error of daily-mean temperature due to photon noise is $\sim 3 \text{ K}$ or less in summer.

time of 1 hour for all the PMC parameters (for all the sites we analyzed) so that the number of independent PMC observations during the first summer season at McMurdo is taken to be 85. Using this standard approach, the error bar of mean PMC altitude is calculated to be 172 m compared to the geophysical variability of 1.59 km as shown in Table 1. Furthermore, because the distribution of PMC altitudes is symmetric and close to Gaussian [Chu *et al.*, 2006; Fiedler *et al.*, 2009], taking the mean centroid altitude and the standard error is an appropriate characterization of the PMC altitudes at each location. If we now calculate a weighted linear fit to the Rothera, McMurdo and South Pole data points, using the standard errors of the mean altitudes quoted in Table 1, the derived slope is $40 \pm 6 \text{ m/deg}$. Multi-year observations at Rothera and South Pole, as well as extensive satellite observations, suggest that the inter-annual variability in PMC altitudes may be several hundred meters or larger. The effect of this long-term component of the geophysical variability is more difficult to minimize by averaging because it is a global phenomenon with a correlation time of one year. Based upon our six different seasons of PMC observations at the South Pole, McMurdo and Rothera, we calculate that the standard deviation of the inter-annual variability in PMC altitudes is less than about 450 m at these SH sites. If the uncertainty contributed by this inter-annual variability is combined with the short-term geophysical variability quoted in Table 1 by taking into account of the number of seasons of observations at each site, then the weighted least-squares estimate of the slope is $40 \pm 19 \text{ m/deg}$. Based upon these three different methods for computing the linear regression fit, we conclude that the best estimate for the slope is 40 m/deg and the uncertainty (standard deviation) lies between 3 and 19 m/deg. Therefore, we believe that the latitudinal dependence of PMC altitude is statistically significant. By collecting more data in subsequent seasons at these three sites, the uncertainty range, especially the worst-case value that is dominated by the estimated inter-annual variability, can be reduced.

[10] As shown by Russell *et al.* [2010] and Chu *et al.* [2003, 2006], despite the geophysical variability such as interannual, seasonal and diurnal variations, the hemispheric

difference of PMC altitude is a robust result. In any given year, the mean PMC altitudes in the SH are always higher than those in the NH. This is a consequence of the differences in the mesopause region between SH and NH. Atmospheric wave activity, which influences the residual meridional circulation and the summertime upwelling over the polar caps, may vary from year to year, contributing to the geophysical variability. However, the solar flux difference between the two hemispheres is the same year after year, because it is determined by the eccentricity of the Earth's orbit around the Sun. We believe that the primary cause of hemispheric difference in PMC altitudes is the 6% more solar flux received during summer by the South Pole than the North Pole. Dynamic adjustment due to the extra solar flux causes the SH mesopause to be located at a higher altitude with stronger upwelling, resulting in a higher altitude of the supersaturation region thus higher PMC altitudes [Chu *et al.*, 2003]. We also believe that the stronger upwelling towards the pole in summer leads to higher PMCs at higher latitudes. These hypotheses can be tested with detailed modeling and additional observational studies.

2.2. Relationship Among Temperature, PMC and Fe Density

[11] To investigate how the seasonal variations of PMC brightness respond to MLT temperature, the daily-mean PMC brightness (β_{total}) is plotted versus the daily-mean Fe temperatures at 90 km in Figure 3. The 90 km altitude is chosen because it is above the PMC occurrence height (avoiding PMC contamination) and close to the peak of the Fe layer, thus yielding the most accurate temperature measurements. Generally the brighter clouds correspond to colder temperatures, and the derived correlation coefficient is -0.76 at 99% confidence level. The bright PMC displays during 15 Jan and 4 Feb occurred when the daily-mean temperatures at 90 km altitude were coldest ($< \sim 150 \text{ K}$) while the weak displays on 21 Dec 2010 and late Jan 2011 correspond to the warmest temperatures ($\sim 170 \text{ K}$). The linear regression line plotted in Figure 3 suggests that on average the daily-mean β_{total} increases by approximately $1.2 \times 10^{-6} \text{ sr}^{-1}$ for each 10 K decrease in daily-mean temperature.

[12] This negative correlation seems to contradict previous findings of the lack of correlation between the mesopause region temperature and PMC occurrence as summarized by Lübken *et al.* [1996]. However, the temperatures reported by Lübken *et al.* [1996] are the instantaneous temperatures around the mesopause, not the daily means reported here. Notice from Figure 3 that PMCs occur even when the daily-mean temperatures at 90 km are well above 150 K because strong wave oscillations in temperature can facilitate PMC formation during the cold phase of the wave. For example, for the event on 28–29 Jan 2011, the daily-mean temperature is $\sim 160 \text{ K}$, but the lidar data clearly show PMC signatures near 85 km for several hours. Figure 4 illustrates the 28-h of continuous observations of the 372 nm Fe density, Fe and PMC data from 374-nm channel, and the Fe temperature. Although the Fe temperatures are quite warm for the majority of the observation hours ($\sim 170 \text{ K}$), cold temperatures occur periodically with a downward phase progression (indicated by tilted dashed lines) and a period of 6.5–7 h (Figure 4c). Such wave signatures also occur in the Fe densities measured from both 372 and 374 nm channels corresponding to the periodic reduction of Fe densities in

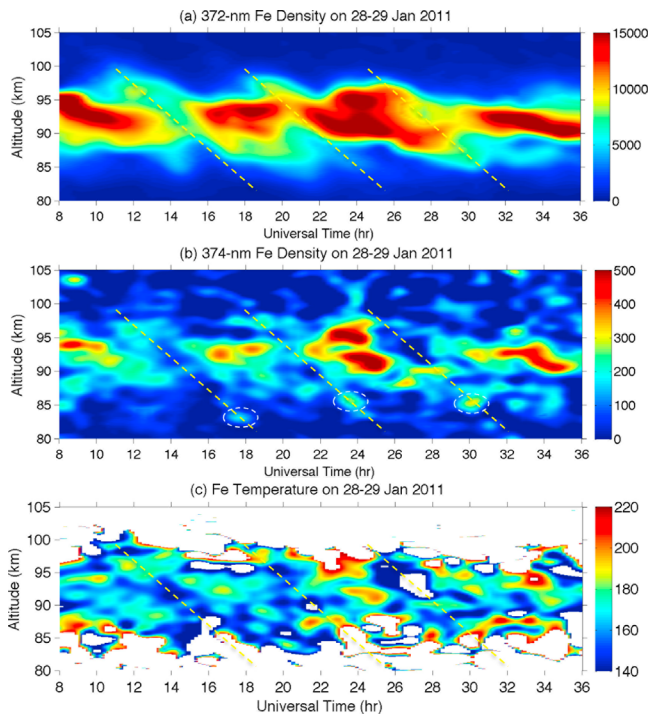


Figure 4. Contour plots of (a) 372-nm Fe density (unit: cm^{-3}) originating from the level of a^5D_4 , (b) 374-nm Fe density (unit: cm^{-3}) originating from the level of a^5D_3 and PMC scattering in equivalent Fe density unit (marked as oval regions), and (c) Fe temperature (unit: K) versus time and altitude on 28–29 January 2011. The dashed lines are used to indicate the downward phase progression of the observed wave. The temperature error is ~ 5 K at 90 km with 1.5 h and 1920 m Hamming smoothing under the full sunlight and summer conditions.

Figures 4a and 4b. A density decrease starts at 13 UT at the 372-nm Fe layer top and propagates downward. By 16 UT, the Fe layer bottom displays a significant density bite-out. Similar features (density reduction and bottom bite-out) repeat twice more through the rest of the observation period. The 374-nm Fe data (Figure 4b) exhibit similar density reductions with the same downward phase progression. Interestingly, at the bottom of this progression, clear PMC layers occur at 83.1 km around 17.5 UT, at 85.5 km around 23.5 UT, and at 85.3 km around 30 UT, as marked with three circles. Such periodic PMC and Fe behaviors are aligned well with the wave-induced temperature oscillations. The cold phase of the temperature oscillation overlaps with the reduction of Fe densities in both channels, and the PMC layers are coincident with the downward progression lines of the cold temperatures, as indicated by the tilted dashed lines in all three panels. The temperature oscillation is large with an amplitude of ~ 20 K, so that the temperature is well below 150 K during the cold phase. The downward phase speed of the wave observed on 28–29 Jan 2011 is ~ 2.4 km/h (i.e., -67 cm/s) and its vertical wavelength is ~ 16 km.

[13] Our lidar data provide direct evidence that PMC formation is facilitated by the cold phase of wave-induced temperature oscillation, as proposed by *Rapp et al.* [2002] in a modeling effort to study the influence of small-scale temperature variations on PMC. In Figure 4, the wave-

induced cold temperatures around 90 km, which is close to the mesopause at ~ 88 km, allow the existence of subvisible ice particles. When the ice crystals are somehow “trapped” in the cold phase through the sedimentation process, they grow into visible size for lidar detection at the bottom of the saturation region around 82–86 km. Besides the case shown in Figure 4, there are other cases in our data where 6–12 h wave oscillations in the temperatures lead to PMC occurrence at the bottom of the downward progression of the cold temperatures. Both horizontal transport and wave-induced vertical wind can contribute to the observed large phase speed. Because the growth of ice particles in the MLT region is much slower than their sublimation, it takes hours for the particles to grow to visible sizes, while a short time to sublimate when the particles experience warm ambient temperatures. PMC ice particles must stay within the cold phase of the temperature; thus, the wave phase speed poses limitations on the sedimentation speed of PMC particles. Ice particles cannot fall too fast or too slow, but have to follow the motion of the cold phase in order to survive and grow to visible sizes.

[14] Trajectories of ice particles are therefore very important as they determine whether the particles can stay within the cold phase for sufficient growth [*Rapp et al.*, 2002]. Since the particle history plays an important role in the PMC formation, the cloud occurrence and brightness are not correlated with the instantaneous temperatures above the clouds as shown in Figure 4, explaining the findings of *Lübken et al.* [1996]. The daily-mean temperatures in Figure 3 represent the background temperatures with the wave-induced oscillations smoothed out. When the background temperatures are colder, the saturated water vapor content is higher. If wave-induced temperature oscillations are also present, then the cold temperatures required for PMC formation will occur during a longer time period. Thus, the probability for survival and growth of ice particles is higher, leading to brighter clouds and more PMC occurrences. This explains the negative correlation of Figure 3.

[15] The periodic reduction of Fe density is well correlated with the cold phase of temperature oscillations induced by waves in Figure 4. Three temperature-related mechanisms contribute to lower Fe densities when temperatures are lower. First, the rates of molecular chemical reactions involving Fe species are temperature dependent and lower temperatures lead to lower Fe densities [*Gardner et al.*, 2005, 2011]. Second, once subvisible and visible ice particles are formed, the uptake of Fe atoms onto the surface of ice particles efficiently removes Fe atoms [*Plane et al.*, 2004]. The “bite-out” of Fe by PMC ice particles is obvious near the bottom of the Fe layers shown as the curvilinear upward displacement of the Fe layer bottom in Figure 4a. Finally, when the species behaves like a passive tracer, upward wave motion causes a decrease of Fe density on the layer bottomsides and results in colder temperatures because of adiabatic cooling of the atmosphere. Consequently, mesospheric metal layers are highly correlated with gravity wave temperature perturbations on the layer bottomsides [*Gardner and Shelton*, 1985].

3. Conclusions

[16] An Fe Boltzmann temperature lidar was successfully deployed to McMurdo, Antarctica, leading to the first

lidar observations of polar mesospheric clouds, meteoric Fe layers and mesopause region temperatures at this high southern latitude in the summer of 2010–2011. The observations are entirely consistent with previous measurements at the South Pole and Rothera which show that PMC altitude increases with increasing latitude at a rate of 40 ± 3 m/deg and that the SH PMCs occur about 1 km higher than their NH counterparts. The PMC brightness at McMurdo falls between the South Pole and Rothera values. These phenomena reflect the differences of the background conditions in the mesopause region between two hemispheres and among different latitudes.

[17] Temperatures in the MLT region play a key role in the overall PMC occurrence and variations in the summer. The daily-mean temperatures at 90 km are anti-correlated with the variations of PMC brightness. We also observed large temperature oscillations induced by long-period (6–12 h) waves with large vertical wavelength (~ 16 km). The cold phase of these temperature oscillations facilitates the formation of PMCs as predicted by Rapp *et al.* [2002] and the concomitant reduction in Fe densities through temperature-dependent molecular chemical reactions and heterogeneous removal of Fe atoms by the subvisible and visible ice particles of PMC as predicted by Plane *et al.* [2004]. These results suggest that the simultaneous and common-volume observations of PMC and temperature in the MLT region over a long period may be used to constrain the growth rate and sedimentation speed of PMC ice particles.

[18] **Acknowledgments.** We acknowledge Adrian J. McDonald and the staff of United State Antarctic Program, McMurdo Research Station, Antarctic New Zealand and Scott Base for their support in the McMurdo lidar campaign. We offer special thanks to Vladimir Papitashvili and Julie Palais at the National Science Foundation for their encouragement and help in deploying the lidar to McMurdo. This project was supported by NSF grant ANT-0839091.

[19] The Editor thanks two anonymous reviewers for their assistance in evaluating this paper.

References

- Chu, X., W. Pan, G. Papen, C. S. Gardner, and J. A. Gelbwachs (2002), Fe Boltzmann temperature lidar: Design, error analysis, and first results from the North and South poles, *Appl. Opt.*, *41*, 4400–4410, doi:10.1364/AO.41.004400.
- Chu, X., C. S. Gardner, and R. G. Roble (2003), Lidar studies of interannual, seasonal, and diurnal variations of polar mesospheric clouds at the South Pole, *J. Geophys. Res.*, *108*(D8), 8447, doi:10.1029/2002JD002524.
- Chu, X., P. J. Espy, G. J. Nott, J. C. Dietrich, and C. S. Gardner (2006), Polar mesospheric clouds observed by an iron Boltzmann lidar at Rothera (67.5°S, 68.0°W), Antarctica from 2002 to 2005: Properties and implications, *J. Geophys. Res.*, *111*, D20213, doi:10.1029/2006JD007086.
- Fiedler, J., G. Baumgarten, and F.-J. Lübken (2009), NLC observations during one solar cycle above ALOMAR, *J. Atmos. Sol. Terr. Phys.*, *71*, 424–433, doi:10.1016/j.jastp.2008.11.010.
- Gardner, C. S., and J. D. Shelton (1985), Density response of neutral atmospheric layers to gravity wave perturbations, *J. Geophys. Res.*, *90*(A2), 1745–1754, doi:10.1029/JA090iA02p01745.
- Gardner, C. S., J. M. C. Plane, W. Pan, T. Vondrak, B. J. Murray, and X. Chu (2005), Seasonal variations of the Na and Fe layers at the South Pole and their implications for the chemistry and general circulation of the polar mesosphere, *J. Geophys. Res.*, *110*, D10302, doi:10.1029/2004JD005670.
- Gardner, C. S., X. Chu, P. J. Espy, J. M. C. Plane, D. R. Marsh, and D. Janches (2011), Seasonal variations of the mesospheric Fe layer at Rothera, Antarctica (67.5°S, 68.0°W), *J. Geophys. Res.*, *116*, D02304, doi:10.1029/2010JD014655.
- Kawahara, T. D., C. S. Gardner, and A. Nomura (2004), Observed temperature structure of the atmosphere above Syowa Station, Antarctica (69°S, 39°E), *J. Geophys. Res.*, *109*, D12103, doi:10.1029/2003JD003918.
- Klekociuk, A. R., R. J. Morris, and J. L. Innis (2008), First Southern Hemisphere common-volume measurements of PMC and PMSE, *Geophys. Res. Lett.*, *35*, L24804, doi:10.1029/2008GL035988.
- Lübken, F.-J., K.-H. Fricke, and M. Langer (1996), Noctilucent clouds and the thermal structure near the Arctic mesopause in summer, *J. Geophys. Res.*, *101*(D5), 9489–9508, doi:10.1029/96JD00444.
- Lübken, F.-J., G. Baumgarten, J. Fiedler, M. Gerding, J. Höffner, and U. Berger (2008), Seasonal and latitudinal variation of noctilucent cloud altitudes, *Geophys. Res. Lett.*, *35*, L06801, doi:10.1029/2007GL032281.
- Plane, J. M. C., B. J. Murray, X. Chu, and C. S. Gardner (2004), Removal of meteoric iron on polar mesospheric clouds, *Science*, *304*, 426–428, doi:10.1126/science.1093236.
- Rapp, M., F.-J. Lübken, A. Müllemann, G. E. Thomas, and E. J. Jensen (2002), Small-scale temperature variations in the vicinity of NLC: Experimental and model results, *J. Geophys. Res.*, *107*(D19), 4392, doi:10.1029/2001JD001241.
- Russell, J. M., III, P. Rong, S. M. Bailey, M. E. Hervig, and S. V. Petelina (2010), Relationship between the summer mesopause and polar mesospheric cloud heights, *J. Geophys. Res.*, *115*, D16209, doi:10.1029/2010JD013852.
- X. Chu, W. Fong, W. Huang, J. A. Smith, Z. Wang, and Z. Yu, Cooperative Institute for Research in Environmental Sciences and Department of Aerospace Engineering Sciences, University of Colorado at Boulder, 216 UCB, Boulder, CO 80309-0216, USA. (xinzha.chu@colorado.edu)
- C. S. Gardner, Department of Electrical and Computer Engineering, University of Illinois at Urbana-Champaign, 1406 W. Green St., Urbana, IL 61811-2918, USA.